

Relationship between the rise width and the full width of gamma-ray burst pulses and its implications in terms of the fireball model

Rui-Jing Lu^{1,2,3*}, Yi-Ping Qin^{1,2} and Ting-Feng Yi²

¹ National Astronomical Observatories/Yunnan Observatory, Chinese Academy of Sciences, P. O. Box 110, Kunming, Yunnan, 650011, P. R. China

² Physics Department, Guangxi University, Nanning, Guangxi 530004, P. R. China

³ The Graduate School of the Chinese Academy of Sciences

Received 2005 month day; accepted 2005 month day

Abstract Kocevski et al. (2003) found that there is a linear relation between the rise width and the full width of gamma-ray burst pulses detected by the BATSE instrument based on their empirical functions. Motivated by this, we investigate the relationship based on Qin et al. (2004) model. Theoretical analysis shows that each of the two quantities, the rise width and the full width of observed pulse, is proportional to $\Gamma^{-2} \Delta\tau_{\theta, \text{FWHM}} \frac{R_c}{c}$, where Γ is the Lorentz factor for the bulk motion, $\Delta\tau_{\theta, \text{FWHM}}$ is a local pulse's width, R_c is the radius of fireballs and c is the velocity of light. We employ the observed pulses coming from four samples to study the relationship and find that: (1) Merely the curvature effect could produce the relationship with the same slope as those derived from Qin et al. (2004) model in the rise width vs. the full width panel. (2) Gamma-ray burst pulses, long or short ones (selected from the short and long GRBs), follow the same sequence in the rise width vs. the full width panel, with the shorter pulses at the end of this sequence. (3) All GRBs may intrinsically result from local Gaussian pulses. These features place constraints on the physical mechanism(s) for producing long and short GRBs.

Key words: gamma rays: bursts – gamma rays: theory – methods: data analysis

1 INTRODUCTION

Although the mechanism underlying the gamma-ray bursts is still an unsolved puzzle, it is generally accepted that the large energies and the short timescales involved require the gamma-rays to be produced in a stage of fireball which expand relativistically (see, e.g., Goodman 1986; paczynski 1986). An individual shock episode gives rise to a pulse in the gamma-ray light curve, and superposition of many such pulses creates the observed diversity and complexity of light curves (Fishman et al. 1994). Therefore, the temporal characteristics of these pulses hold the key to the understanding of the prompt radiation of gamma-ray bursts. It is generally believed that some well-separated individual pulses represent the fundamental constituent of GRB time profiles (light curves) and appear as asymmetric pulses with a fast rise and an exponential decay (FRED), and many pulses have FRED-like shapes.

What result in the observed light curves? According to Ryde & Petrosian (2002), the simplest scenario accounting for the observed GRB pulses is to assume an impulsive heating of the leptons and a subsequent cooling and emission. In this scenario, the rising phase of the pulse, which is referred to as the dynamic time, arises from the energizing of the shell, while the decay phase reflects the cooling and its timescale. However, in general, the cooling time for the relevant parameters is too short to explain the pulse durations and the resulting cooling spectra are not consistent with observation (Ghisellini et al. 2000). As shown by Ryde & Petrosian (2002), this problem could be solved when the curvature effect of the expanding fireball surface is taken into account.

The diversities of gamma-ray light curves in morphology could be interpreted within the standard fireball model (Rees & Mészáros 1992), and the observed FRED structure was found to be interpreted by the curvature effect as the observed plasma moves relativistically towards us and appears to be locally isotropic (e.g., Fenimore et al. 1996, Ryde & Petrosian 2002; Kocevski et al. 2003, hereafter Paper I). Several investigations on modeling pulse profiles have previously been made (e.g., Norris et al. 1996; Lee et al. 2000a, 2000b; Ryde & Svensson 2000; Ryde & Petrosian 2002; Borgonovo & Ryde 2001; Paper I), they derived several flexible functions to describe the profiles of individual pulses based on empirical or semi-empirical relations. E.g., as derived in detail in Paper I, a FRED pulse can be well described by the equation (22) or (28). Using this model, they found that there is a linear relationship between the full width at half-maximum, often denoted FWHM, and the rise width of gamma-ray burst pulses detected by the BATSE instrument (see Fig. 10 in paper I), and the same result can be found in the gamma-ray burst pulses detected by the anti-coincidence shield of the spectrometer (SPI) of INTEGRAL (see Fig. 5a Ryde et al. 2003).

Qin (2002) has derived in detail the flux function based on the model of highly symmetric expanding fireball, where the Doppler effect of the expanding fireball surface is the key factor to be concerned, and then with this formula, Qin (2003) studied how emission and absorption lines are affected by the effect. Recently, Qin et al. (2004) presented the formula in terms of count rates. Based on this model, some relations, a power law relationship between the observed pulse width and energy (Qin et al. 2005a), an anti-correlation between the power law index and the local pulse width (Jia et al. 2005), and correlations between spectral lags and some physical parameters, such as Lorentz factor and the fireball radius (Lu et al. 2005a), have emerged. At the same time, some characteristics have been found, such as a reverse S-feature curve in the decay phase (Qin et al. 2005b) and an inflection from concavity to convexity in the rising phase (Lu et al. 2005b) of the light curve determined by equation (21) in Paper II. The Combination of these knowledge is suggestive of a potential relationship between the rise width and the full width of the observed pulse, which motivates us to investigate the relationship found by Kocevski et al. based on Qin model and explore its implications in terms of the fireball model.

Although the origins of short GRBs and long GRBs are not yet clear, it is generally suggested that short GRBs are likely to be produced by the merger of compact objects while the core collapse of massive stars is likely to give rise to long GRBs (see Zhang & Mészáros 2004; Piran 2005). Many properties, such as luminosity, $\langle V/V_{max} \rangle$, the angular distribution, the energy dependence of the duration, and the hard-to-soft spectral evolution, even pulses profile of short GRBs, are also similar to those of long GRBs (e.g., Schmidt 2001; Ramirez-Ruiz & Fenimore 2000; Lamb et al. 2002; Ghirlanda et al. 2004; Cui et al. 2005), which indicate that the GRBs appear to have the same emission mechanism and possibly different progenitors for long and short bursts. Motivated by this, we also investigate the temporal structure of narrow pulses with durations shorter than 1 s (FWHM) from short GRBs and long GRBs.

This paper is organized as follows. In section 2, we investigate the temporal characteristics of light curves of GRBs based on Qin model. In section 3, we examine the relationship between the rise width and the full width of observational pulses and explore its possible implication in terms of the fireball model. Discussion and conclusions will be presented in the last section.

2 THE THEORETICAL ANALYSIS

As derived in detail in paper II, the expected count rate of the fireball within frequency interval $[\nu_1, \nu_2]$ can be calculated with

$$C(\tau) = \frac{2\pi R_c^3 \int_{\tau_{\theta,\min}}^{\tau_{\theta,\max}} \tilde{I}(\tau_\theta) (1 + \beta \tau_\theta)^2 (1 - \tau + \tau_\theta) d\tau_\theta \int_{\nu_1}^{\nu_2} \frac{g_{0,\nu}(\nu_{0,\theta})}{\nu} d\nu}{hcD^2 \Gamma^3 (1 - \beta)^2 (1 + k\tau)} \quad (1)$$

In above formula, τ_θ is a dimensionless relative local time defined by $\tau_\theta \equiv c(t_\theta - t_c)/R_c$, where t_θ is the emission time in the observer frame, called local time, of photons emitted from the concerned differential surface ds_θ of the fireball (θ is the angle to the line of sight), t_c is a constant which could be assigned to any values of t_θ , and R_c is the radius of the fireball measured at $t_\theta = t_c$; Variable τ is a dimensionless relative time defined by $\tau \equiv [c(t - t_c) - D + R_c]/R_c$, where D is the distance of the fireball to the observer, and t is the observation time; $\tilde{I}(\tau_\theta)$ represents the development of the intensity magnitude in the observer frame, called as a local pulse function; $g_{0,\nu}(\nu_{0,\theta})$ describes the rest frame radiation mechanisms; And $k \equiv \beta/(1 - \beta)$. At the same time, the integral limits $\tilde{\tau}_{\theta,\min}$ and $\tilde{\tau}_{\theta,\max}$ are determined by $\tilde{\tau}_{\theta,\min} = \max\{\tau_{\theta,\min}, (\tau - 1 + \cos \theta_{\max})/(1 - \beta \cos \theta_{\max})\}$ and $\tilde{\tau}_{\theta,\max} = \min\{\tau_{\theta,\max}, (\tau - 1 + \cos \theta_{\min})/(1 - \beta \cos \theta_{\min})\}$, where $\tau_{\theta,\min}$ and $\tau_{\theta,\max}$ are the lower and upper limits of τ_θ confining $\tilde{I}(\tau_\theta)$, and θ_{\min} and θ_{\max} are determined by the concerned area of the fireball surface, and then the radiation is observable within the range of $(1 - \cos \theta_{\min}) + (1 - \beta \cos \theta_{\min})\tau_{\theta,\min} \leq \tau \leq (1 - \cos \theta_{\max}) + (1 - \beta \cos \theta_{\max})\tau_{\theta,\max}$.

Formula (1) suggests that, light curves of sources depend mainly on Γ , $\tilde{I}(\tau_\theta)$ and $g_{0,\nu}(\nu_{0,\theta})$. Observation suggests that the common radiation form of GRBs is the so-called Band spectrum function (Band et al. 1993) which was frequently, and rather successfully, employed to fit the spectra of the sources (see, e.g., Schaefer et al. 1994; Ford et al. 1995; Preece et al. 1998, 2000), therefore we take in this paper the Band function as the rest frame radiation form. And the rise width and the full width of light curves depend on the two factors of sources, Γ and $\tilde{I}(\tau_\theta)$.

In this paper, we use τ_r and τ_{FWHM} refer to the rise width and the full width of light curves corresponding to variable τ , and t_r and t_{FWHM} to those corresponding to variable t , respectively. In the same way, we use $\Delta\tau_{\theta,\text{FWHM}}$ refer to the FWHM of a local pulse corresponding to variable τ_θ , and $\Delta t_{\theta,\text{FWHM}}$ to that corresponding to variable t_θ .

For the sake of simplicity, we first employ a local pulse with a power law rise and a power law decay to study this issue, which is written as

$$\tilde{I}(\tau_\theta) = I_0 \left\{ \begin{array}{ll} \left(\frac{\tau_\theta - \tau_{\theta,\min}}{\tau_{\theta,0} - \tau_{\theta,\min}} \right)^\mu & (\tau_{\theta,\min} \leq \tau_\theta \leq \tau_{\theta,0}) \\ \left(1 - \frac{\tau_\theta - \tau_{\theta,0}}{\tau_{\theta,\max} - \tau_{\theta,0}} \right)^\mu & (\tau_{\theta,0} < \tau_\theta \leq \tau_{\theta,\max}) \end{array} \right. . \quad (2)$$

Where $\tau_{\theta,0}$ and μ are constants. The FWHM of this local pulse would be $\Delta\tau_{\theta,\text{FWHM}} = (1 - 2^{(-1/\mu)})(\tau_{\theta,\max} - \tau_{\theta,\min})$. The relationships between τ_r , τ_{FWHM} and Γ , and that between τ_r , τ_{FWHM} and $\Delta\tau_{\theta,\text{FWHM}}$ for the light curves determined by equation (1) are plotted in Fig. 1, and presented in Fig. 2 is the relationship between the τ_r and the τ_{FWHM} of the light curves.

Figure 1 shows that the τ_r and τ_{FWHM} decrease with the Lorentz factor following $\tau_r \propto \Gamma^{-2}$ and $\tau_{\text{FWHM}} \propto \Gamma^{-2}$, and they increase with $\Delta\tau_{\theta,\text{FWHM}}$ following $\tau_r \propto \Delta\tau_{\theta,\text{FWHM}}$ for every value of $\Delta\tau_{\theta,\text{FWHM}}$, and $\tau_{\text{FWHM}} \propto \Delta\tau_{\theta,\text{FWHM}}$ when $\Delta\tau_{\theta,\text{FWHM}} \geq 1$. Thus we

obtain

$$\tau_r = k_1 \Gamma^{-2} \Delta \tau_{\theta, \text{FWHM}} = k_1 p, \quad (3)$$

$$\tau_{\text{FWHM}} = k \Gamma^{-2} \Delta \tau_{\theta, \text{FWHM}} = k p \quad (\Delta \tau_{\theta, \text{FWHM}} \geq 1), \quad (4)$$

where $p = \Gamma^{-2} \Delta \tau_{\theta, \text{FWHM}}$. $k_1 = 0.597 \pm 0.006$ and $k = 1.335 \pm 0.036$ for this local pulse. Study reveals that each of the two quantities, τ_r and τ_{FWHM} , is proportional to p , but independent of Γ or $\tau_{\theta, \text{FWHM}}$.

Considering the relation between τ and t , we get from (3) and (4) that

$$t_r = k_1 p \frac{R_c}{c}, \quad (5)$$

$$t_{\text{FWHM}} = k p \frac{R_c}{c} \quad (\Delta \tau_{\theta, \text{FWHM}} \geq 1). \quad (6)$$

We find from the left panel in Fig. 2 that the τ_r increases linearly with the τ_{FWHM} when we take $\Delta \tau_{\theta, \text{FWHM}} = \text{constant}$ and $\Gamma = \text{variable}$. We thus perform a linear least square fit to the two quantities, and have $\log(\tau_r) = A + B \log(\tau_{\text{FWHM}})$ for a certain value of $\Delta \tau_{\theta, \text{FWHM}}$. There are almost the same slopes of “B” (i.e. $B = 1.0$) for different values of $\Delta \tau_{\theta, \text{FWHM}}$, whereas the value of “A” changes from -1.981 to -0.526 when $\Delta \tau_{\theta, \text{FWHM}}$ changes correspondingly from 0.001 to 0.1, and there is an upper limit value of $A \approx -0.40$ when $\Delta \tau_{\theta, \text{FWHM}} \geq 1$, thus a dead line can be found when $\Delta \tau_{\theta, \text{FWHM}} \geq 1$, i.e., $\log(\tau_r) = -0.404 + 1.00 \times \log(\tau_{\text{FWHM}})$. (for all situations of fitting, their correlation coefficient $R > 0.999$ and the number of the data $N=27$.)

According to equations (6) and (7) in Paper II, one could find that the photons that observer receives at different observation time τ emit from the different surface of fireball when $\Delta \tau_{\theta, \text{FWHM}} < 1$, so that the profiles of the light curves determined by formulas (1) are affected by $\Delta \tau_{\theta, \text{FWHM}}$. Whereas when $\Delta \tau_{\theta, \text{FWHM}} \geq 1$, the photons reaching the observer at different observation time τ come from the same whole surface of the fireball, in this situation, the profiles of the light curves don't change with $\Delta \tau_{\theta, \text{FWHM}}$. This analysis is supported by the fact that the τ_r is sensitive to the $\Delta \tau_{\theta, \text{FWHM}}$, but the τ_{FWHM} isn't significantly affected by the $\Delta \tau_{\theta, \text{FWHM}}$, when $\Delta \tau_{\theta, \text{FWHM}} < 1$, in fact in this case the τ_{FWHM} slightly decreases with the $\Delta \tau_{\theta, \text{FWHM}}$, and when $\Delta \tau_{\theta, \text{FWHM}} \rightarrow 0$, the local pulse becomes a δ one, and the τ_{FWHM} would be determined by equation (44) in Paper II. However when $\Delta \tau_{\theta, \text{FWHM}} \geq 1$, each of the two quantities, τ_r and τ_{FWHM} , linearly increases with the $\Delta \tau_{\theta, \text{FWHM}}$ with the same slope (see the right panel in Fig. 1). Which naturally explains why one could find a dead line in the $\tau_r - \tau_{\text{FWHM}}$ panel when $\Delta \tau_{\theta, \text{FWHM}} \geq 1$.

When changing frequency interval from $100 \leq \nu / \nu_{0,p} \leq 300$ to $25 \leq \nu / \nu_{0,p} \leq 50$, or to other frequency interval, and repeating the same work as above, we find that the results don't change significantly, and the dead line is not sensitive to frequency interval.

We study other forms of local pulses, such as $\mu = 1, 3$ of equation (2), an exponential rise and exponential decay pulse, a Gaussian pulse, and a rectangle pulse, and so on,

and find that the equation (3) - (6) hold for all local pulses we investigate, and there are different values of k_1 and k for different local pulse forms (see Table 1). For every local pulse form, a dead line can be found when $\Delta\tau_{\theta,FWHM} \geq 1$. The dead lines of the six local pulses, $\log(\tau_r) = (-0.563 \pm 0.005) + (1.015 \pm 0.002)\log(\tau_{FWHM})$ for local exponential pulse, $\log(\tau_r) = (-0.520 \pm 0.009) + (1.027 \pm 0.003)\log(\tau_{FWHM})$ for local Gaussian pulse, $\log(\tau_r) = (-0.450 \pm 0.003) + (1.005 \pm 0.001)\log(\tau_{FWHM})$ for $\mu = 3$ of equation (2), $\log(\tau_r) = (-0.404 \pm 0.006) + (1.007 \pm 0.001)\log(\tau_{FWHM})$ for $\mu = 2$ of equation (2), $\log(\tau_r) = (-0.318 \pm 0.005) + (1.011 \pm 0.001)\log(\tau_{FWHM})$ for $\mu = 1$ of equation (2), and $\log(\tau_r) = (-0.221 \pm 0.011) + (1.027 \pm 0.003)\log(\tau_{FWHM})$ for local rectangle pulse, are presented in the right panel in Fig. 2.

Studies show that, for all kinds of local pulse forms, the slopes of their dead lines are always equal to 1.0, but there are different intercepts for different local pulse forms in the $\tau_r - \tau_{FWHM}$ panel. The intercept could therefore become an indicator of the local pulse form. We also note that the dead line of local rectangle form is the upper limit one for all local pulse forms (i.e., the intercept of a dead line for any local pulse forms would never exceed -0.20), which might be a criterion to check if the temporal behaviors of gamma-ray burst pulses do result from the contributions from the Doppler effect.

3 RELATIONSHIP BETWEEN THE RISE TIME AND THE WIDTH OF OBSERVATIONAL PULSES

Kocevski et al. (2003) found that there is a linear correlation between the rise width vs. the full width of gamma-ray burst pulses provided by the BATSE instrument on board the CGRO (Compton Gamma Ray Observatory) spacecraft. For the sake of convenience of comparision with those obtained theoretically above, unlike Kocevski et al., we here investigate the temporal structures of the light curves of 2nd and 3rd channels based on their sample, respectively, which we call sample 1. As they pointed out that a power-law rise model can better describe the majority of the FRED pulses, so we measure the t_r and the t_{FWHM} of the pulses by fitted with the equation of (22) in their paper. The results are presented in Fig. 3.

Fig. 3 shows that the t_r increase linearly with the t_{FWHM} of the observed pulses. We perform a linear least square fit at 1σ confidence level to the two quantities, and have $\log(t_r) = (-0.531 \pm 0.022) + (1.045 \pm 0.029)\log(t_{FWHM})$ with a linear correlation coefficient of 0.973 and a chance probability of $p < 10^{-4}$ for the 2nd channel, and $\log(t_r) = (-0.492 \pm 0.029) + (1.031 \pm 0.024)\log(t_{FWHM})$ with a linear correlation coefficient of 0.980 and a chance probability of $p < 10^{-4}$ for the 3rd channel. The results show that the two sequence in the $t_r - t_{FWHM}$ panel have almost the same intercepts and slopes within their error. Intriguingly, one find that the slope is equal to the one obtained theoretically

above, which indicates that the observed results are well consistent with those predicted by Qin model.

We thus may come to the conclusions: (1) Merely the curvature effect can produce the relationship in the $t_r - t_{\text{FWHM}}$ panel which is independent of any frequency interval. (2) The gamma-ray burst pulses most probably arise from local Gaussian form because the sequences in the $t_r - t_{\text{FWHM}}$ panel is closed to the dead line of local Gaussian form. Note that the differences between the two panels, $\tau_r - \tau_{\text{FWHM}}$ and $t_r - t_{\text{FWHM}}$, don't affect the comparison (See section (4)).

To further demonstrate these conclusion, we choose another sample, call sample 2, based on gamma-ray burst pulses detected by HETE-2 instrument. Like Kocevski, we select pulses from the HETE-2 burst home page (<http://space.mit.edu/HETE/Bursts/>) with the simple criteria that pulses behave clean, well distinguished FRED-like form, thus 12 pulses could be available in our sample 2. We measure the t_r and t_{FWHM} of these pulses with the same methods as above. And the results are presented in Fig. 4. We perform a linear least square fit to the two quantities with the same methods adopted in Fig. 3, and obtain $\log(t_r) = (-0.494 \pm 0.065) + (1.012 \pm 0.087)\log(t_{\text{FWHM}})$ with a linear correlation coefficient of 0.960 and a chance probability of $p < 10^{-4}$ for the band B, and $\log(t_r) = (-0.504 \pm 0.059) + (1.088 \pm 0.078)\log(t_{\text{FWHM}})$ with a linear correlation coefficient of 0.976 and a chance probability of $p < 10^{-4}$ for the band C. The results are well consistent with those obtained from Fig. 3, which further testifies that the sequences in the $t_r - t_{\text{FWHM}}$ plane is independent of any frequency interval.

The first two smaller standard deviations of the four intercepts in the two sample from the ones of the six dead lines obtained above theoretically are 0.043 for local Gaussian pulse and 0.120 for local exponential pulse, which indicates that these four sequences are very closed to the dead line of the local Gaussian pulse and implicate that these observed pulses may arise from local Gaussian pulses. The conclusion is only a preliminary one which needs to be confirmed by larger samples in the future.

As shown in Fig. 3 and 4, all pulses, which are selected from long bursts, are longer than 0.5 s. Norris et al. 2001 pointed out that short bursts with $T_{90} < 2.6s$ have different temporal behaviors compared with long bursts. Whether or not short pulses and long ones follow the same sequence in the $t_r - t_{\text{FWHM}}$ plane and behave the same temporal behavior? motivated by this, we select 6 short pulses, call sample 3, from the 64 ms count data of 532 short GRBs, and 23 short pulses (shorter than 1 s), call sample 4, from long GRBs with the same criteria adopted in sample 2. These short and long GRBs are detected by the BATSE instrument. We repeat the same work as above, and the results are plotted in the left panel in Fig. 5.

We find from the left panel in Fig. 5 that, all pulses (selected from short and long GRBs) follow the same sequence in the $t_r - t_{\text{FWHM}}$ plane, with the shorter pulses at the end of this sequence, which show that short pulses (or bursts) behave the same temporal

behaviors as long pulses, the only difference is that the quantity of p (see equation of (3) or (4)) of short pulse is smaller than the one of long pulse.

4 DISCUSSION AND CONCLUSIONS

All analyses in this paper are based on formula (1), which is based on the case of a fireball expanding isotropically with a constant Lorentz factor, $\Gamma > 1$. In fact, the symmetry of expansion matters only over angles the order of a few times Γ^{-1} , and beaming prevents us from observing other regions of the shell. The formula (1) is suitable for describing light curves of spherical fireballs or uniform jets. When considering a uniform jet and taking $\theta_{\max} = \Gamma^{-1}$ in the formula (1), we measure the τ_r and τ_{FWHM} of the resulting light curves. They show no difference from those of the spherical geometry, which indicate that the relationships in the τ_r - τ_{FWHM} plane are independent of gamma-ray burst pulses coming from either spherical fireballs or uniform jets.

It is an ubiquitous trend that indexes of spectra of many GRBs are observed to vary with time (see Preece et al. 2000). We wonder how the relationship would be if the rest frame spectrum develops with time. As Preece et al. (2000) pointed out that the typical fitted value distributions for the low energy spectral index (α) is $-1.5 \sim -0.3$, the high energy spectral index β is $-2 \sim -3$. Therefore here some sets of typical values of the indexes such as $(-1.5, -2)$, $(-0.3, -3)$ and $(-0.8, -2.5)$ would be employed to investigate the relationship. Calculations show that the two quantities, τ_r and τ_{FWHM} , are not significantly affected by the rest frame radiation form.

We find that, owing to the Doppler effect of the fireball surface (or the curvature effect), for any local pulse form, the width of the light curve would always be $t_{\text{FWHM}} = k\Gamma^{-2}\Delta\tau_{\theta,\text{FWHM}}\frac{R_c}{c}$ (There are different values of k for different local pulse forms, see Table 1). As derived in detail in Paper II, the width of the light curve of the local δ function pulse would be $\tau_{\text{FWHM}} \simeq \frac{\sqrt{2}-1}{2}\Gamma^{-2}\Delta\tau$ (see (48) in Paper II), where $\Delta\tau$ is the interval of the observable time of the local δ function pulse, i.e., $\Delta\tau = 1 + \beta\tau_{\theta,0}$. When considering the relationship between τ and t , and taking $\tau_{\theta,0} = 0$, we obtain $t_{\text{FWHM}} \simeq \frac{\sqrt{2}-1}{2}\Gamma^{-2}\frac{R_c}{c} \simeq 2s(\frac{R_c}{10^{15}\text{cm}})(\frac{\Gamma}{10^2})^{-2}$, which would be the lower limit of the width of light curves for any local pulse form. Because of the relativistic beaming of the moving radiating particles, only the emission from a narrow cone with an opening angle of Γ^{-1} is observed, Ryde & Petrosian (2002) obtained that the curvature timescale resulting from relativistic effects is $\tau_{\text{ang}} = 1.7s(\frac{R_c}{10^{15}\text{cm}})(\frac{\Gamma}{10^2})^{-2}$ (See (5) in their paper). Even as they pointed out that this is a lower bound for the observed duration of a pulse. Thus it can be seen that the curvature timescale and the lower limit of the width of light curves are comparable.

According to the equations (3) and (6), we know that the only difference between the two panels, $t_r - t_{\text{FWHM}}$ and $\tau_r - \tau_{\text{FWHM}}$, is that the different observed pulses resulting from

the same Γ and $\Delta\tau_{\theta,\text{FWHM}}$ but from different values of R_c would be only corresponding to one point in the $\tau_r - \tau_{\text{FWHM}}$ plane; but in the $t_r - t_{\text{FWHM}}$ plane these observed pulses would be corresponding to different points as they come from different values of R_c , and these different points must be on a line with the slope, $B=1.0$. However the intercepts of the light curves in the two panels dependent only on both forms and widths of their corresponding local pulses.

It is widely accepted that gamma-ray bursts arise from the internal shocks at a distance of $R_c \sim 10^{13} - 10^{17} \text{ cm}$ in the scenario of standard fireball model (see Rees & Mészáros 1992, 1994; Mészáros & Rees 1993, 1994; Mészáros 1995; Katz 1994; Paczynski & Xu 1994; Sari & Piran 1997; Piran 1999; Spada et al. 2000; Ryde & Petrosian 2002; and Piran 2005). To compare theoretic conclusions with the observed results in the $t_r - t_{\text{FWHM}}$ plane, we merge the left panel in Fig. 5 into the right panel in Fig. 2 by applying equation (5) and (6) and taking $R_c = 3 \times 10^{15} \text{ cm}$, and the results could be plotted in the right panel in Fig. 5. The results are in good agreement with those predicted by Qin model. We notice that the all observed pulses are under the dead line of local Gaussian form within their errors.

As shown above, local pulses' widths, $\Delta\tau_{\theta,\text{FWHM}} \geq 0.1$, for most of observed pulses. Applying the relationship between τ_θ and t_θ , we obtain that $\Delta t_{\theta,\text{FWHM}} \geq 0.1 \frac{R_c}{c}$. Because taking $\tau_{\theta,\text{min}} = 0$ (i.e., $t_{\theta,\text{min}} = t_c$) in above analysis, we know that R_c at that time is the radius of fireball at which radiation begins to emit, which may correspond to the stage the fireball become optically thin and photons can escape freely. And the fact that $\Delta\tau_{\theta,\text{FWHM}} \geq 0.1$ indicates that local pulse's width is not less than 1 order of the time scale the fireball expands to become optical thin for most of observed pulses, and its implication is not clear now because we don't know what result in the local pulses yet.

In all, we come to the following conclusions: (1) Merely the curvature effect could produce the observed relationship between t_r and t_{FWHM} . (2) Both long pulses and short ones follow the same sequence in the $t_r - t_{\text{FWHM}}$ plane. If all observed pulses come from the same radius of fireballs (especially for the pulses in a burst), the shorter pulses have smaller value of p (Here $p = \Gamma^{-2} \Delta\tau_{\theta,\text{FWHM}}$), which might implicate that short pulses come from larger Γ and narrower local pulses than long pulses, and short bursts come from largest Γ and narrowest local pulses than long bursts, this is a reasonable result if short GRBs are likely to be produced by the merger of compact objects while long GRBs result from the core collapse of massive stars. (3) All GRBs may arise intrinsically from local Gaussian pulses, and these local pulses' widths, $\Delta\tau_{\theta,\text{FWHM}}$, would not be less than 0.1, which is in agreement with those found in Qin et al. (2005b). (4) The observed pulses deviated down from the the dead line of local Gaussian pulse would arise from the narrower local pulses (i.e., smaller than 1), and the shorter the local pulses, the more obvious the deviation feature. However we suspect that there will not be such a observed

pulse far deviated up from the dead line of the local Gaussian pulse in the $t_r - t_{\text{FWHM}}$ plane if it arises from a local Gaussian pulse in terms of the fireball model.

These features above may provide constraints on intrinsic emission mechanism responsible for GRBs.

Acknowledgements This work was supported by the Special Funds for Major State Basic Research Projects (“973”) and National Natural Science Foundation of China (No. 10273019 and 10463001).

References

Band D., Matteson J., Ford L. et al., 1993, *ApJ*, 413, 281
 Borgonovo L., Ryde F., 2001, *ApJ*, 548, 770
 Cui X. H., Liang E. W., Lu R. J., 2005, *Chin. J. Astron. Astrophys.*, 5, 151
 Fenimore E. E., Madras C. D., Nayakshin, S., 1996, *ApJ*, 473, 998
 Fishman G. J., Meegan C. A., Wilson R. B. et al., 1994, *ApJS*, 92, 229
 Ford L. A., Band D. L., Matteson J. L. et al., 1995, *ApJ*, 439, 307
 Goodman J. 1986, *ApJ*, 308, L47
 Ghirlanda G., Ghisellini G., Celotti A., 2004, *A&A* 422L, 55G
 Ghisellini G., Celotti A., Lazzati D., 2000, *MNRAS*, 313, L1
 Jia L. W., Qin Y. P., *ApJL*, in press, astro-ph/0505309
 Katz J. I., 1994, *ApJ*, 422, 248
 Kocevski D., Ryde F., Liang E., 2003, *ApJ*, 596, 389 (Paper I)
 Lamb D. Q., Ricker G. R., Atteia J. L. et al. 2002, *ApJ*, submitted, astro-ph/0206151
 Lee A., Bloom E. D., Petrosian V., 2000a, *ApJS*, 131, 1
 Lee A., Bloom E. D., Petrosian V., 2000b, *ApJS*, 131, 21
 Lu R. J., Qin Y. P., Zhang Z. B. et al., 2005a, *MNRAS*, Submitted, astro-ph/0509287
 Lu R. J., Qin Y. P., 2005b, *MNRAS*, Submitted, astro-ph/0508537
Mészáros P., Rees M. J., 1993, *ApJ*, 405, 278
Mészáros P., Rees M. J., 1994, *MNRAS*, 269, L41
Mészáros P., 1995, in *Procs. 17th Texas Symp. Rel. Astroph.* (NY Acad. Sci., New York), 759, 440
 Norris J. P., Nemiroff R. J., Bonnell J. T. et al., 1996, *ApJ*, 459, 393
 Paczynski B., 1986, *ApJ*, 308, L43
 Paczynski B., Xu G., 1994, *ApJ*, 427, 708
 Piran T., 1999, *Phys. Rep.*, 314, 575
 Piran T., 2005, *Reviews of Modern Physics*, 76, 1143
 Preece R. D., Pendleton G. N., Briggs M. S. et al., 1998, *ApJ*, 496, 849
 Preece R. D., Briggs M. S., Mallozzi R. S. et al., 2000, *ApJS*, 126, 19
 Qin Y. P., 2002, *A&A*, 396, 705
 Qin Y. P., 2003, *A&A*, 407, 393
 Qin Y. P., Zhang Z. B., Zhang F. W. et al., 2004, *ApJ*, 617, 439 (Paper II)
 Qin Y. P., Dong Y. M., Lu R. J. et al., 2005a, *ApJ*, in press, astro-ph/0411365
 Qin Y. P., Lu R. J., 2005b, *MNRAS*, 362, 1085Q
 Ramirez-Ruiz E., Fenimore E. E., 2000, *ApJ*, 539, 712
 Rees M. J., *Mészáros* P., 1992, *MNRAS*, 258, 41
 Rees M. J., *Mészáros* P., 1994, *ApJ*, 430, L93
 Ryde F., Svensson R., 2000, *ApJ*, 529, L13
 Ryde F., Petrosian V., 2002, *ApJ*, 578, 290
 Ryde F., Borgonovo L., Larsson S. et al., 2003, *A&A*, 411, L331
 Schaefer B. E., Teeguarden B. J., Fantasia S. F. et al., 1994, *ApJS*, 92, 285

Table 1 The Coefficients For Equation (3) And (4)

Local pulse forms	k_1	k
$\mu = 1$ of equation(2)	0.412 ± 0.003	0.827 ± 0.022
$\mu = 2$ of equation(2)	0.597 ± 0.006	1.335 ± 0.036
$\mu = 3$ of equation(2)	0.717 ± 0.009	1.718 ± 0.041
An exponential rise and decay pulse	0.306 ± 0.001	2.006 ± 0.122
A Gaussian pulse	0.650 ± 0.007	2.782 ± 0.149
A rectangle pulse	0.149 ± 0.001	0.318 ± 0.013

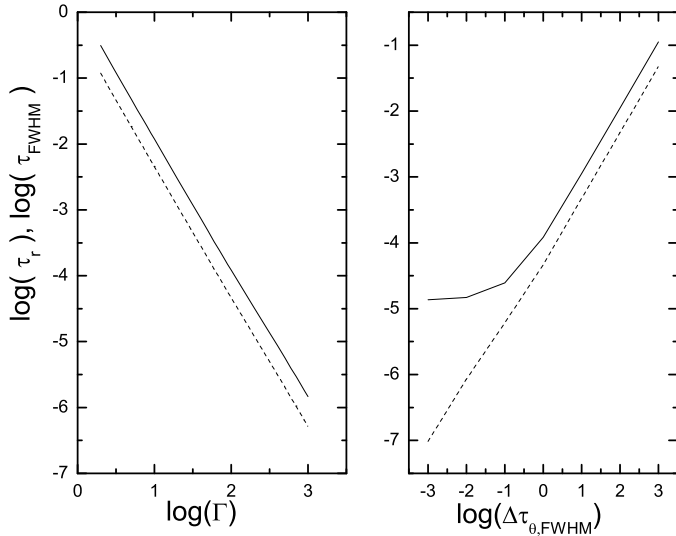


Fig. 1 Relationships between τ_r , τ_{FWHM} and Γ (Left panel) and that between τ_r , τ_{FWHM} and $\Delta\tau_{\theta,\text{FWHM}}$ (Right panel) for the light curves determined by equation (1), where a band function rest frame radiation form with $\alpha_0 = -1$ and $\beta_0 = -2.25$, within the frequency range of $100 \leq \nu/\nu_{0,p} \leq 300$, is adopted, and we take $2\pi R_c^3 I_0/hcD^2 = 1$, $\mu = 2$, $\tau_{\theta,\text{min}} = 0$, $\theta_{\text{min}} = 0$, $\theta_{\text{max}} = \pi/2$, $\Delta\tau_{\theta,\text{FWHM}} = 1$ (Left panel), and $\Gamma = 100$ (Right panel). The solid and the dash line represent the τ_{FWHM} and the τ_r of light curves in both panels, respectively.

Schmidt M., 2001, APJ, 559, L79

Sari R., Piran T., 1997, MNRAS, 287, 110

Spada M., Panaitescu A., Mészáros P., 2000, ApJ, 537, 824

Zhang B., Mészáros P., 2004, IJMPA, 19, 2385Z

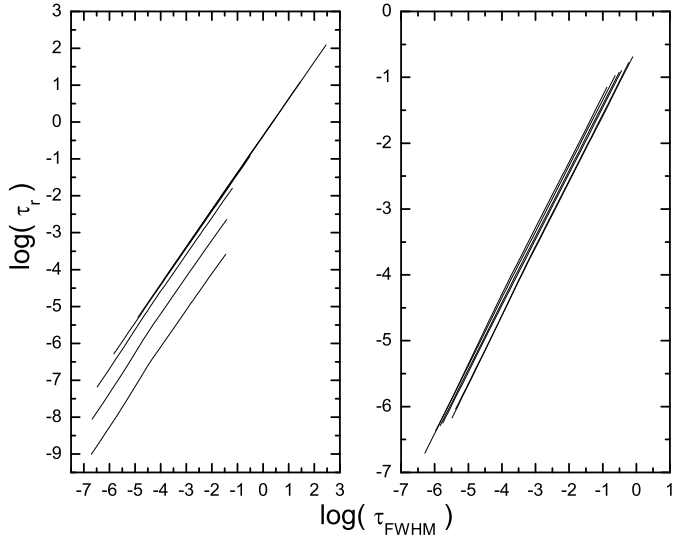


Fig. 2 Relationships between τ_r and τ_{FWHM} for the light curves determined by equation (1). Left panel: We take $\Gamma=2$ to 1000 for different values of $\Delta\tau_{\theta,\text{FWHM}}$. The solid lines from the bottom to the top represent $\Delta\tau_{\theta,\text{FWHM}}=0.001, 0.01, 0.1, 1, 10, 100$, and 1000, respectively. (note: when $\Delta\tau_{\theta,\text{FWHM}} \geq 1$, their corresponding lines overlap each other.) Right panel: the dead lines of the six local pulse forms: the solid lines from the bottom to the top represent local exponential rise and exponential decay pulse, local Gaussian pulse, local power law pulse $\mu=3, 2, 1$ of equation (2) and local rectangle pulse, respectively. Other parameters are the same as those adopted in Fig. 1.

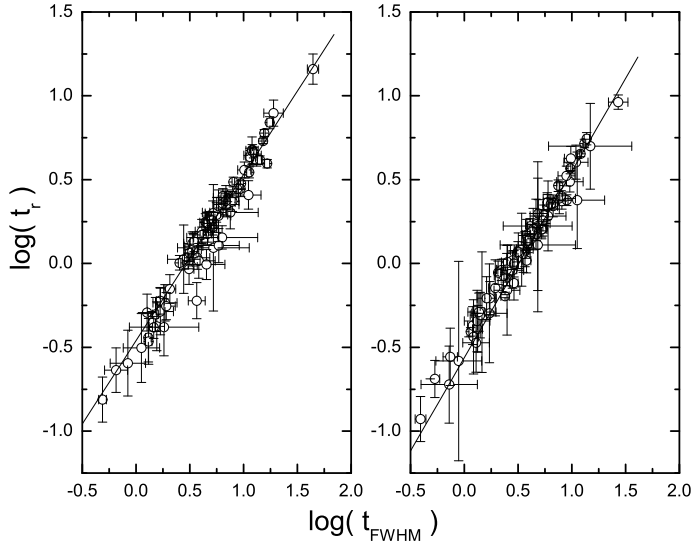


Fig. 3 Relationships between t_r and t_{FWHM} for the observed pulses based on sample 1. The left and the right panel present the pulses of the 2nd channel and the 3rd channel, respectively. The two solid lines are the fit lines of their data.

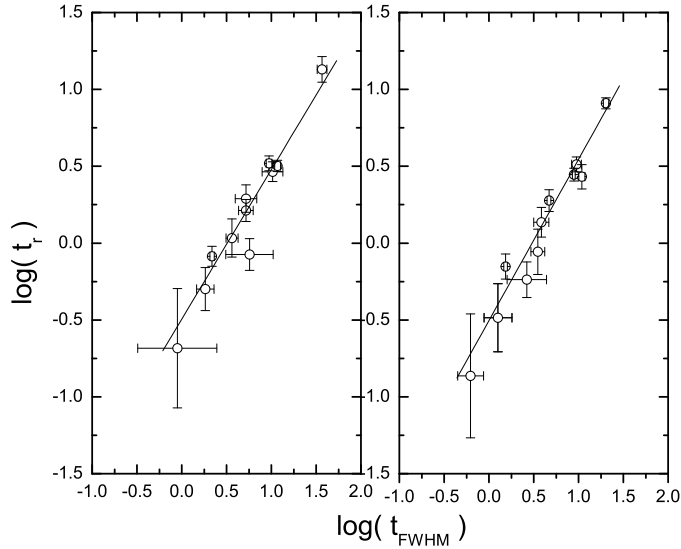


Fig. 4 Relationships between t_r and t_{FWHM} for the observed pulses based on sample 2. The left panel and the right panel present the pulses of the band B (7-40 keV) and C (30-400 keV), respectively. The two solid lines are the fit lines of their data.

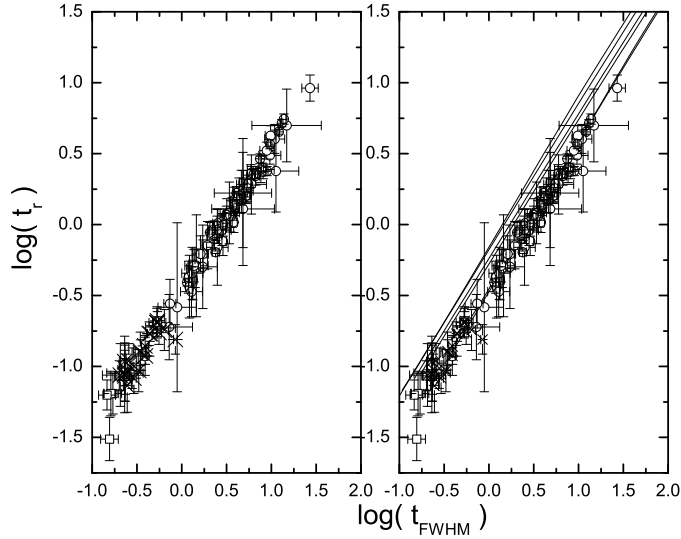


Fig. 5 Relationships between t_r and t_{FWHM} for the observed pulses. Left panel presents the observed pulses of the 3rd channel based on sample 1, 3 and 4. The open circle, the open rectangle and the cross present the pulses of sample 1, 3 and 4, respectively. Right panel is a combination of the left panel and the right panel in Fig. 2, where we take $R_c = 3 \times 10^{15} \text{ cm}$.